J Mater Sci (2007) 42:9131–9136
DOI 10.1007/s10853-007-1932-z

Effect of flexure induced transverse crack and self-healing on chloride diffusivity of reinforced mortar

Mustafa Şahmaran

Received: 23 February 2007 / Accepted: 11 June 2007 / Published online: 28 July 2007

Abstract Cracks in reinforced concrete are unavoidable. Durability is of increasing concern in the concrete industry, and it is significantly affected by the presence of cracks. The corrosion of reinforcing steel due to chloride ions in deicing salts or sea-water is a major cause of premature deterioration of reinforced concrete structures. Although, it is generally recognized that cracks accelerate the ingress of chlorides in concrete, a lack of consensus on this subject does not yet allow reliable quantification of their effects. The present work studies the relationship between crack widths and chloride diffusivity. Flexural load was introduced to generate cracks of width ranging between 29 and 390 μm. As crack width was increased, the effective diffusion coefficient was also increased, thus reducing the initiation period of corrosion process. For cracks with widths less than 135 μm, the effect of crack widths on the effective diffusion coefficient of mortar was found to be marginal, whereas for crack widths higher than 135 μm the effective diffusion coefficient increased rapidly. Therefore, the effect of crack width on chloride penetration was more pronounced when the crack width is higher than 135 μm. Results also indicate that the relation between the effective diffusion coefficient and crack width was found to be power function. In addition, a significant amount of self-healing was observed within the cracks with width below 50 μm subjected to NaCl solution exposure. The present research may provide insight into developing design criteria for a durable concrete and in predicting service life of a concrete structures.

M. Şahmaran (✉)
Department of Civil Engineering, Gaziantep University,
Gaziantep 27310, Turkey
e-mail: sahmaran@gantep.edu.tr

Introduction

Corrosion of steel reinforcement is one of the major causes of deterioration leading to shortened service life of reinforced concrete structures. The principal cause of corrosion in reinforced concrete structures is chloride ion attack. Concrete may be exposed to chloride by sea-water or de-icing salts. Generally, after casting concrete, a passivation film is formed surrounding the steel bars that protect them from corrosion initiation. However, when a sufficient chloride concentration, a threshold value, is reached on the steel surface, the passivation film disrupts and the corrosion process is initiated. When the steel bar starts to corrode, the volume of corrosion product exerts pressure on the concrete resulting in spalling of the concrete cover. Moreover, the cross-section of reinforcing bar is diminished, thus reducing the load carrying capacity of the concrete member.

Extensive research has been conducted over the past decades to study transport properties of concrete and numerous service life prediction models have been introduced. While these models correlate with laboratory investigations, they usually fail to accurately predict service life of real structures. Their common disadvantage is that all predictions are carried out considering a sound concrete [1]. Concrete has very low tensile strength, and thus, it is impossible to keep concrete from cracking during its service life. Cracking is usually a result of various physical and chemical interactions (thermal stress, shrinkage, creep, attacks of aggressive chemicals, external mechanical loads, etc.) between concrete and environment, and it may develop at different stages throughout the life of the structure. Cracks most often tend to be tapered or V-shaped due to flexural loads; however, parallel-wall cracks are also common in concrete structures under direct tension. Once initiated, cracks create pathways for oxygen

and water transportation, thus, facilitating the ingress of deleterious species, such as chlorides, carbonates, sulfates and acids into concrete.

The role of the crack differs according to mechanism of transportation. Permeation, diffusion, and absorption are three different transportation mechanisms for a fluid and deleterious species to move through a concrete [2]. The main driving force behind permeation is the presence of a hydraulic pressure gradient. The transport of chloride in concrete by means of permeation may occur in concrete with a high intensity of cracks and defects. Absorption, driven by capillary pore suction, is the predominant transport process when the unsaturated concrete is exposed to chloride solution. Diffusion is the most commonly studied transport process of chloride ions. When the saturated concrete is exposed to a chloride solution, a chloride concentration gradient is created between the concrete element surface and the pore solution. In this case, diffusion will be the predominant driving mechanism of chloride transport. The chloride always diffuses into zones with smaller chloride concentrations. Therefore, depending upon the conditions, mass transfer may be driven by one or a combination of these three mechanisms.

The influence of cracking and crack widths on the transport property of concrete is a subject that has received much debate. In the past, considerable research and discussion has been devoted to this topic without arriving at a general consensus. One of the main reasons of the diversity (lack of consensus) of results obtained from these different studies can be attributed to the variety of experimental methods to create these cracks. A comparison of diffusion coefficients for cracked and uncracked concrete shows an increase in the diffusion coefficient for cracked concrete by one or two orders of magnitude, with wider cracks resulting in higher values [3]. Chloride diffusion in concrete pre-cracked under 3-point bending loading was also studied by Gowripalan et al. [4]. Prisms were pre-loaded up to 0.3 mm crack width. The experiment showed that the apparent chloride diffusion coefficient is larger in the tensile than in the compression zone. Mangat and Gurusamy studied the influence of cracks on chloride diffusion of steel fiber reinforced concrete [5]. Crack of widths ranging between 70 and 1,080 μm were produced on prism specimens and exposed to cycles of splash and tidal zone marine exposure. The authors concluded that crack widths larger than 500 μm have more pronounced influence on chloride intrusion while crack widths less than 200 μm appeared to have nearly no effect on chloride intrusion. The relationship between crack width and chloride diffusivity was also examined by Rodriguez and Hooton [6]. The authors concluded that the diffusion coefficient of concrete is not influenced by the occurrence of cracks. However, in that work the influence of the artificially created, roughly constant width cracks on

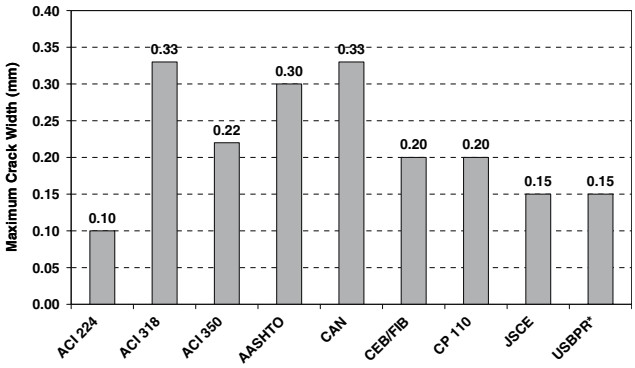

Fig. 1 Comparison of allowable crack widths: severe exposure (*: maximum crack width at level of reinforcement) [10–18]

chloride ingress into concrete was studied. Konin et al. performed research on penetration of chloride ions in relation to microcracking resulting from flexural load [7]. The results indicated that chloride penetration rate increases with increasing density of microcracks. Moreover, a linear relationship between the chloride apparent diffusion coefficient and the applied tensile load was established, which is in agreement with research by Francois and Arliguie [8]. It was noted that chloride diffusion coefficients and concrete strengths are also linearly related. Aldea et al. performed rapid chloride permeability tests on normal and high strength concrete samples pre-cracked under feedback-controlled splitting tensile test, with crack width up to 400 μm [9]. It was concluded that cracks less than 200 μm had no effect on chloride conductivity, while cracks between 200 and 400 μm resulted in higher chloride conductivity. A summary of maximum allowable crack widths at the tensile face of reinforced concrete structures for severe environment in various codes and technical committee is shown in Fig. 1 [10–18]. As seen from Fig. 1, the strictest requirement is specified by ACI 224.

In the present research, experimental work was conducted on reinforced mortar beam specimens preloaded to different deformation levels to produce different crack widths. The cracked specimens were then exposed to sodium chloride solution. The performance of cracked and uncracked reinforced mortar specimens in terms of chloride penetration profile and depth, and effective diffusion coefficient was compared. The main objective of this study was to quantify how transverse cracking caused by flexural loading influences the chloride transport properties of mortar, which may be used to predict changes in durability performance under service conditions.

Materials and mixture proportions

The mixture proportion of the mortar specimens are summarized in Table 1. To eliminate any variation due to

Table 1 Mixture properties of mortar

	Mortar
W/C	0.485
Cement (C)	1.00
Sand/cement (by mass)	2.75
7-day compressive strength (MPa)	28.7
28-day compressive strength (MPa)	35.9

coarse aggregate, mortar mixture was intentionally used to determine the effect of crack width on the diffusion coefficient of chloride. The mortar mixture included only Portland cement (ASTM Type-I) as a binder. The sand used for mortar is river sand with an average size of 0.6 mm. A standard water to cement ratio (W/C) of 0.485 was selected in accordance with ASTM C109. The compressive strength test results of mortar mixtures are also listed in Table 1. The compressive strength was computed as an average of three Ø75 × 150-mm cylinder specimens.

Test specimen preparation and testing

Chloride ion profiles and diffusion coefficient of mortar were evaluated in accordance with AASHTO T259-80 [19]. About 355.6 × 50.8 × 76.2 mm prisms were produced for salt ponding test. According to AASHTO T259, it is not necessary to place steel bars in mortar to determine chloride ion profiles and diffusion coefficient of uncracked mortar. In this experimental study, however, chloride ion profiles and diffusion coefficient of cracked and uncracked mortar were compared. It is very difficult to achieve cracks of varying controlled widths for mortar specimens. For this reason, each mortar prism was reinforced with three levels of steel mesh reinforcement made of 1 mm diameter in a 6 mm grid. Mortar specimens were compacted using a vibrating table. The prisms were demolded at the age of 24 h, and moisture cured at 95 ± 5% RH, 23 ± 2 °C for 14 days. The specimens were then air cured at 50 ± 5% RH, 23 ± 2 °C until the age of 42 days for testing. At the age of 42 days, the prisms were pre-cracked using 4-point bending test to obtain different crack widths. The ponding test was carried out with the pre-cracked specimens in the unloaded state. A small amount of crack closure occurred on unloading. To account for this, all crack width measurements are conducted in the unloaded stage. The widths of the crack were measured on the surface of the specimens by an optical microscope. In this study, cracks due to flexural loads were not identical in widths on the inside as on the surface and crack widths were narrower at the deeper level of prism specimens than at the surface (V-shaped crack). The average width of the resulting crack

Table 2 Crack widths, numbers and depths of pre-loaded reinforced mortar prisms

Beam deformation (mm)	Average crack widths (μm)	Crack depth (mm)	Crack number
0.38	29.4	18.7	1
0.52	49.0	28.1	1
0.61	102.9	36.6	1
0.86	210.7	47.3	1
0.98	283.0	63.2	1
1.10	392.0	73.4	1

was obtained through measurement of the crack widths on the surface at five different points. In addition to crack widths, the optical microscope was also used to establish the extent to which the crack had traveled up from the tension face of the beam towards the compression face (crack depth). After the bending load application, one single crack was present in the mortar specimens. Table 2 shows the pre-loaded beam deformation (BD) value, their corresponding average crack widths (CW), depths and number of cracks for prism specimens. Two prisms were also tested without pre-loading for control purpose. After load application, plexiglass was used around the side surface of the prism to build an embankment for holding chloride solution on the exposed surface of prisms. At the age of 43 days, a 3% of NaCl solution was ponded on the cracked surface of prisms. In order to retard the evaporation of solution, aluminum sheet was used to cover the top surface of the specimens. After 30 days of ponding, the salt solution was removed from the prism surface and samples were taken from each specimen for measuring chloride concentration with depth. In the case of initially unloaded specimens, ponding test was also conducted after 90 days NaCl solution exposure in accordance with AASHTO T259-80 [19].

After 30 days sodium chloride exposure, it was found that chloride penetration concentrates at where the pre-crack was located, and the penetration depth was deep, approximately 40–75 mm depending on the crack width and crack depth of the specimen. At each cracked zone (Fig. 2), two sample holes were dry drilled for chloride analysis at various depths by using a 15 mm diameter rotary drill. Potentiometric titration method was used to determine the total chloride concentration in the powdered mortar samples [20].

The chloride profiles were then input into a statistical and curve-fitting software. Equation 1, Crank's solution to Fick's second law, was fitted to the data [21]. The regression analysis yielded the values of the effective diffusion coefficient (D_e) and surface chloride concentration (C_s) for each specimen

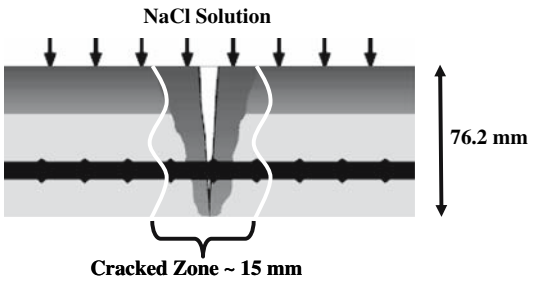

Fig. 2 Locations of the sampling for chloride profiling

$$C_{(x,t)} = C_s\left[1 - \mathrm{erf}\left(\frac{x}{2\sqrt{D_e t}}\right)\right], \quad (1)$$

where $C_{(x,t)}$, chloride concentration at time t at depth x (wt.% of mortar); C_s, surface chloride concentration (wt.% of mortar); erf( ), error function; x, distance from mortar surface (m); t, exposure time (s); and D_e, effective chloride diffusion coefficient (m^2/s).

This equation would perfectly describe the diffusion process of chlorides when no other transport mechanism of chloride ions (absorption and permeation) is present. However, this is not the case in real field conditions. In this experimental study, the coefficient of diffusion found by regression analysis of chloride profiles using Eq. 1 is referred to as effective diffusion coefficient (D_e) which includes the combined transport mechanics (absorption, permeation, diffusion, etc.). The D_e calculated in this study helps describe the shape of the chloride profiles and forms a reasonable basis of comparing the diffusion properties of cracked and uncracked mortar specimens.

Experimental results and discussion

The chloride concentration profiles of uncracked mortar from the ponding test of prism specimens after 28 and 90 days of exposure, with the values of effective diffusion coefficients (D_e) and coefficient of determinations (R^2) as determined by regression analysis, are shown in Fig. 3. The coefficient of determination (R^2) represents the correlation between the Eq. 1 and the actual data. A perfect fit of the equation and the data will have R^2 equal to one. The value of D_e for uncracked mortar after 30 days sodium chloride solution exposure is 2.34×10^{-11} m^2/s, which reduces sharply to 1.09×10^{-11} m^2/s after 90 days sodium chloride solution exposure. This exposure age dependence of effective diffusion coefficient is due to the continuing cement hydration process which is beneficial in reducing pore sizes and densifying matrix [5].

The chloride concentration profiles of cracked mortar, which were exposed to NaCl solution, are shown in Fig. 4.

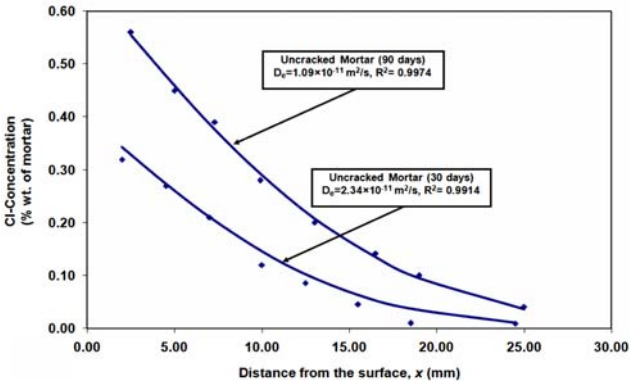

Fig. 3 Chloride profiles of uncracked mortar prisms after 30 and 90 days in 3% NaCl solution

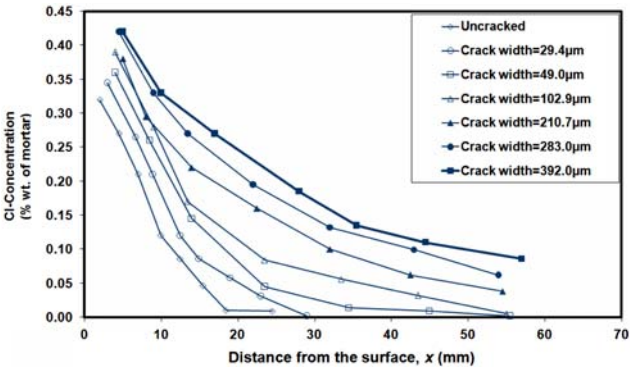

Fig. 4 Chloride profiles of mortar prisms in cracked zone after 30 days NaCl solution exposure

The chloride concentration profiles of initially uncracked specimens cured in the same environment and of same age are also included in this figure. The chloride contents at different depths from the exposed surface were determined after 30 days exposure to chloride environment. The chloride content in the cracked zone decreased with increasing crack depth because cracks generated in beams under bending load have crack width reducing along its length (V-shaped crack). In all cases, chloride concentrations increase with increasing crack width at all depths from the top of the mortar specimens. The increase is fairly high at crack widths especially larger than 200 μm for mortar specimens. These conclusions are also consistent with previous research findings [5].

The effective chloride diffusion coefficients of prisms calculated by using Fick's second law are given in Table 3. The effective diffusion coefficient of pre-cracked mortar specimens is calculated on the crack zone, because, for cracked specimens, the majority of chloride penetration occurs through the crack and not uniformly through the material area. As expected, this table clearly demonstrates

Table 3 Chloride ponding test—effective diffusion coefficient

Beam deformation (mm)	Average crack widths (μm)	Effective diffusion coefficient ($m^2/s \times 10^{-11}$)
–	–	2.34
0.38	29.4	2.82
0.52	49.0	3.70
0.61	102.9	5.47
0.86	210.7	14.19
0.98	283.0	21.00
1.10	392.0	32.36

that effective diffusion coefficient increased as the crack width of the mortar specimens increased.

Figure 5 shows the relationship between the crack width and the effective diffusion coefficient of chloride ions through a crack on mortar specimens which were exposed to 30 days NaCl solution. At the crack, salt solution may fill the crack and diffusion may also occur from the crack plane [4]. This is evident from the high chloride concentrations measured along the depth of crack. As seen from Fig. 5, two different trends were observed. The effective diffusion coefficient increased with increases in the crack width and was almost constant when the crack width was between 29.4 and 102.9 μm. As shown in Fig. 5, a critical crack width occurs at approximately 135 μm. The effective diffusion coefficient is significantly increased when the crack width was larger than 135 μm as illustrated in Fig. 5. It also appears that the effective diffusion coefficient of mortar has the form of power function of the crack width. The relationship between crack width and chloride diffusivity was also examined by other researchers. Despite the numerous tests and experimental methods used, a consensus on relation between crack width and the coefficient of diffusion has never been reached. Some authors found some increase of the diffusivity with a multiplicative factor in the range of 1–10 [3, 22]. Others found no effect or a decrease of the diffusion, but in that work the influence of the artificially created, roughly constant width cracks on chloride ingress into concrete was studied [6]. However, in real field condition, crack generally does not constant in widths on the inside as on the surface and the shape of the crack is generally V-shaped. The experimental methods to create cracks, the methods used to measure chloride transport properties, the methods used to measure chloride contents and the reactivity of the chemical element with the solid body are the main reasons of diversity obtained from different studies [23].

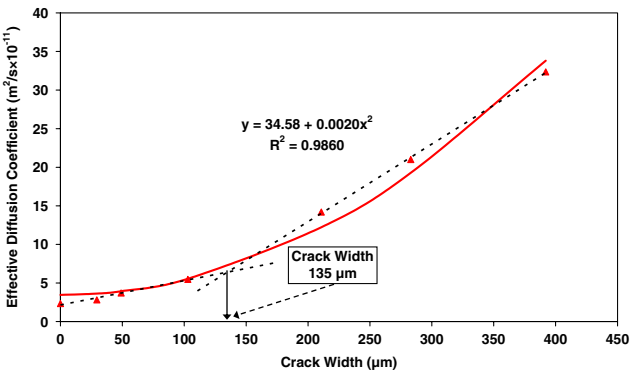

Fig. 5 Diffusion coefficient vs. crack width for mortar deformed under bending load

Due to the high diffusion coefficient, mortar beams reinforced with three layers of steel mesh, pitting corrosion was also observed in the steel mesh of specimens having crack widths of 392 μm after 30 days NaCl solution exposure. Therefore, cracks can reduce the service life of reinforced concrete structures by accelerating the initiation of corrosion especially when the crack width is larger than 135 μm.

The self-healing of cracks should also be taken into account when crack width is small. Based on experimental results, Evardsen, and Reinhardt and Jooss proposed that cracks with width below 0.1 mm can be closed by a self-healing process [24, 25]. In the case of pre-cracked mortar specimens that have crack width less than 50 μm exposed to salt solution, a distinct white traces at the mortar surface was visible at the end of 1 month exposure period (Fig. 6a). X-ray diffractogram of the crack surface have shown the formation of calcite ($CaCO_3$) as practically an exclusive cause of self-healing (Fig. 6b). This white deposit on the crack surface easily blocked the flow path when the crack width was less than 50 μm. These results show that the transportation process of chlorides along the crack path of mortar specimens that have crack width less than 50 μm is considerably slower due to self-healing and tight crack width.

Conclusion

Chloride diffusivity of mortar with different crack widths was evaluated. After bending load application, a single V-shaped crack is present on the mortar specimens. The relation between the effective diffusion coefficient and crack width was found to be power function. As crack width was increased, the effective diffusion coefficient was also increased, thus reducing the initiation period of corrosion process. For crack widths less than 135 μm, the effect of crack widths on the effective diffusion coefficient of mortar was found to be marginal, whereas for crack widths higher than 135 μm the effective diffusion coefficient increased rapidly. Therefore, the effect of crack width on chloride penetration was more pronounced when the

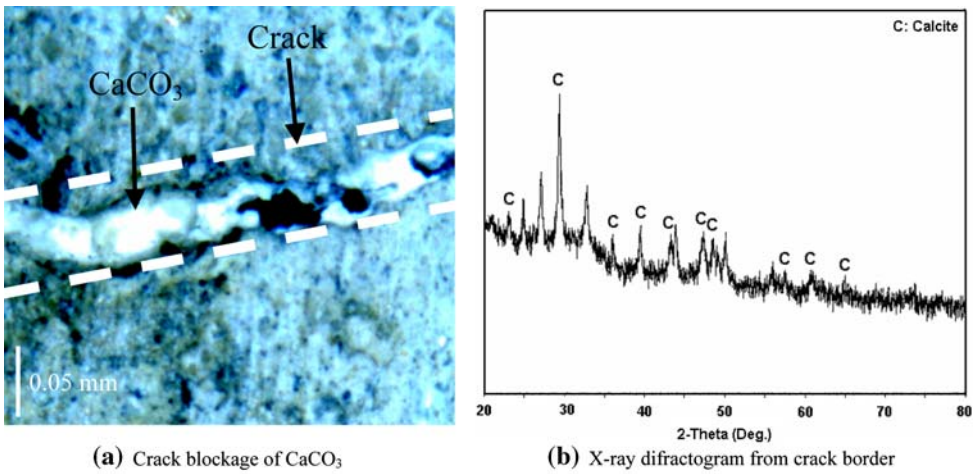

Fig. 6 Self-healing products in mortar specimens after 30 NaCl solution exposure (crack width = 49 μm)

(a) Crack blockage of $CaCO_3$ **(b)** X-ray difractogram from crack border

crack width is higher than 135 μm. Additionally, cracks width less than 50 μm, a significant amount of self-healing was observed within the cracks subjected to 30 days sodium chloride solution. Ultimately, the formation of self-healing products slows the rate of chloride penetration through the crack zone and further reduces the effective diffusion coefficient of cracked mortar specimens.

References

1. De Schutter G (2000) In: Durability of marine concrete structures damaged by early age thermal cracking. International RILEM Workshop on Life Prediction and Aging Management of Concrete Structures, Cannes, France, Oct. 16–17, 2000
2. Poulsen E (2006) Diffusion of chloride in concrete: theory and application. Taylor & Francis, London
3. Raharinaivo A, Brevet P, Grimaldi G, Pannier G (1986) In: Relationship between concrete deterioration and reinforcing-steel corrosion. Durability of building materials, vol 4, pp 97–112
4. Gowripalan N, Sirivivatnanon V, Lim CC (2000) J Cement Concrete Res 30(5):725
5. Mangat PS, Gurusamy K (1987) J Cement Concrete Res 17(3):385
6. Rodriguez OG, Hooton RD (2003) ACI Mater J 100(2):120
7. Konin A, Francois R, Arliguie G (1998) Mater Struct 31(209):310
8. Francois R, Arliguie G (1999) Mag Concrete Res 51(2):143
9. Aldea CM, Shah SP, Karr A (1999) J Mater Civil Eng 11(3):181
10. ACI Committee 224R (2001) Control of cracking in concrete structures, ACI 224-01. American Concrete Institute, Detroit, Michigan
11. ACI Committee 318 (1995) Building code requirements for reinforced concrete, ACI 318-95. American Concrete Institute, Detroit, Michigan
12. ACI Committee 350 (1989) Environmental engineering concrete structures, ACI 350R-89. American Concrete Institute, Detroit, Michigan
13. AASHTO (1998) LRFD bridge design specifications, 2nd ed. American Association of State Highway and Transportation Officials, Washington, DC
14. CAN3-A23.3-M84 (1984) Design of concrete structures for buildings. Canadian Standards Association, Ontario
15. CEB-FIB Model Code 1990 (1993) CEB information report no. 213/214. Comite Euro-International DuBeton, Lausanne
16. Code of practice for the structural use of concrete – part 1. Design, materials and workmanship. British Standards Institution Publication CP 110, London, England, May 1977
17. Standard specification for design and construction of concrete structures – part 1 (Design). Japan Society of Civil Engineers, SP-1, Tokyo, Japan, 1986
18. U.S. Bureau of Public Roads – Bridge Division (1967) Strength and serviceability criteria – reinforced concrete bridge members. U.S. Department of Transportation, Washington, DC
19. AASHTO (2001) Standard method of test for resistance of concrete to chloride ion penetration, AASHTO T 259-80. AASHTO, USA
20. AASHTO (2001) Standard method of test for sampling and testing for chloride ion in concrete and concrete raw materials, AASHTO T 260-97. AASHTO, USA
21. Crank J (1975) The mathematics of diffusion, 2nd edn. Oxford University Press, London
22. Tognazzi C, Ollivier J-P, Carcasses M, Torrenti J-M (1998) In: Petit Ch, Pijaudier-Cabot G, Reynouard JM (eds) Couplage Fissuration-Dégradation Chimique des Matériaux Cimentaires: Premiers Résultats sur les Propriétés de Transfert, Ouvrages, géomate´riaux et interactions. Herme's, Paris, pp 69–84
23. Gerard B, Reinhardt HW, Breysse D (1997) In: Reinhardt HW (ed) Measured transport in cracked concrete, penetration and permeability of concrete. RILEM, France, Report 16, pp 123–153
24. Evardsen C (1999) ACI Mater J 96(4):448
25. Reinhardt HW, Jooss M (2003) J Cement Concrete Res 33(7):981